Numerical Simulation Analysis of the Influence of Entrance Wind Speed on the Wind Speed Distribution of Coal Mine Tunnel Sections

Yahu Yao[1, 2]

[1]Chongqing Research Institute of China Coal Technology and Engineering Group Crop., Chongqing, 400037, China
[2]State Key Laboratory of the Gas Disaster Detecting, Preventing and Emergency Controlling, Chongqing, 400037, China

Abstract: In order to further accurately obtain the wind speed of coal mine tunnels and achieve intelligent ventilation, taking the Wuhushan coal mine tunnel as the research object, the COMSOL Multiphysics numerical simulation software was used to simulate and analyze the influence of inlet wind speed on the wind speed distribution on the tunnel section, and the wind speed distribution law of the semi circular arch tunnel section under different inlet wind speed conditions was obtained. The research results indicate that the wind speed contour is basically parallel to the tunnel wall, and the wind speed gradient near the tunnel wall is large, while the wind speed gradient in the middle of the tunnel is small. The thickness of the boundary layer decreases with increasing wind speed. The ratio of the maximum wind speed to the average wind speed of the tunnel section is approximately 1.2125. The distance between the average wind speed line of the semi circular arch tunnel and the roof is 10.76%~11.02% of the tunnel height, and the error between the simulation results and theoretical calculation results is within 4%. The research results provide strong support for precise measurement of the average wind speed at fixed points in coal mine underground tunnels.

Keywords: Mine ventilation, Tunnel cross-section, Tunnel wind speed, Inlet wind speed, Numerical simulation.

1. Introduction

As coal mining enters a new era of safety and intelligence, intelligent technology is deeply integrated with the coal industry, and intelligent control of coal mine roadway ventilation is an important guarantee for achieving efficient production in mines [1-3]. The ventilation system of coal mines is an open and complex system. The intelligent ventilation system of coal mines can ensure the quality of air supply in real time based on changes in underground ventilation parameters, and meet the air demand of mines during normal and disaster periods. It is an indispensable and important component of the intelligent construction of coal mines [4-5]. Therefore, exploring the distribution pattern of wind speed at the cross-section of coal mine tunnels is the key to accurately settling the intelligent ventilation network in mines.

In recent years, domestic and foreign scholars have conducted in-depth research on the distribution law of wind speed at the cross-section of coal mine tunnels using numerical simulation methods. Hao Yuanwei et al. [6] used CFD software to conduct three-dimensional numerical simulation of the airflow field in mine tunnels, revealing the distribution characteristics of airflow velocity in different forms of tunnels, and analyzing the relationship between wind speed at monitoring points and average wind speed. Li Yong et al. [7] selected the Yongchuan coal mine excavation face and the nearby 50 m roadway area as the research object, and used CFD software to simulate and analyze the airflow field in the roadway. The results showed that the overall airflow velocity in the excavation face and roadway is divided into high-speed airflow area and low-speed airflow area based on the outlet of the air duct. Zhao Wenhua [8] applied commercial fluid analysis software CFX to numerically simulate the ventilation process of a single head tunnel in a certain mine excavation, and obtained the distribution of airflow in the tunnel. Lu Guangli et al. [9] studied the variation law of airflow in tunnels at different turning angles, and used Fluent numerical simulation software to construct 12 models. The study showed that the variation law of airflow in tunnels remained consistent under different wind speeds, while the average wind speed point position in the tunnel remained fixed. Wang Hanfeng et al. [10] used Fluent numerical simulation software to simulate the airflow field of the tunnel model under different conditions, and obtained the relationship between the average wind speed line position and the tunnel cross-section. Sun Liang et al. [11] simulated the distribution law of wind speed in large cross-section tunnels using FLUENT software and found that as the cross-sectional area increased, the influence of the area of the anemometer on the wind speed measurement value became smaller and smaller.

At present, the monitoring of tunnel wind speed and air volume in Wuhushan Coal Mine mainly relies on manual wind measurement and sensor monitoring. The use of traditional ventilation parameter monitoring equipment cannot meet the requirements of intelligent and accurate measurement of ventilation parameters, leading to misleading management and decision-making of ventilation technology. Therefore, it is necessary to further study the distribution law of wind speed in the cross-section of the Wuhushan Coal Mine roadway, accurately obtain the wind speed in the roadway, and achieve intelligent ventilation. Based on the above, this paper uses COMSOL Multiphysics numerical simulation software to study the distribution law of wind speed in the tunnel section under different inlet wind speeds, providing support for the rapid and accurate measurement of tunnel wind speed and the implementation of intelligent ventilation in Wuhushan Coal Mine.

2. Overview of the Mine

Wuhushan Mining Company is affiliated with Shenhua Wuhai Energy Co., Ltd. The company is located in the southern part of the Wuda mining area in the northern section of Helan Mountain, Inner Mongolia Autonomous Region. The geographical coordinates are 106°34′~106°38′ E and 39°27′~39°33′ N. The north-south direction of the mine field is 4.5km long, and the east-west direction is 2.5km long, with an area of approximately 8.08km^2. There are currently 8 minable coal seams in the mine field (9 #, 10 #, 12 #, 2 #, 13 #, 15 #, 16 #, 17 #). The coal seams in the mine field are present in a monoclinic structure, with a strike approximately north-south and an inclination towards the east. The dip angle of the coal seams is between 3° and 15°.

The mine is currently mining 9 #, 10 #, and 12 # layers of coal, with two panels arranged for mining. The 9 # and 10 # coal seams are jointly arranged as panels (9 # layer panels), and the 12 # coal seam is separately arranged as a single panel. Each panel is equipped with tape up mountain, track up mountain, return air up mountain, centralized return air roadway, and return air inclined shaft. The working face is arranged along the direction of the coal seam, and the comprehensive mechanized retreating roof caving method is adopted for mining. 95% of the tunnels achieve comprehensive excavation technology.

The mine adopts a zone extraction ventilation system. There are currently 4 air intake shafts, including main inclined shaft, auxiliary inclined shaft, fourth floor reverse inclined shaft, and pedestrian inclined shaft for air intake, and two return air shafts, namely the ninth floor return air shaft and the twelfth floor return air shaft. Two explosion-proof counter rotating axial flow fans BD-II-8 № 26(Power 2×315KW, rated maximum air volume 8800m^3/min, negative pressure 2570Pa) and BDK-III-24(Power 2×160KW, rated maximum air volume 5800m^3/min, negative pressure 1600Pa) are installed in the two return air shafts. The total intake air volume of the mine is about 12445 m^3/min, the total return air volume is about 12587 m^3/min, the negative pressure is 2577 Pa, the ventilation level hole is 5.04 square meters, and the maximum ventilation flow is 7780 meters.

3. Numerical Simulation Scheme and Parameter Selection

Based on the actual conditions of Wuhushan Coal Mine, the cross-sectional size of the semi-circular arch roadway has been determined to be 4m×3m, with tunnel models all measuring 100m in length, and the COMSOL Multiphysics numerical simulation software is used to study the effect of inlet wind speed on the distribution of wind speed in the tunnel cross-section. When modeling, the length of the roadway model is selected in the X direction, the height of the roadway model in the Y direction, and the width of the roadway model in the Z direction. The numerical simulation geometric model is shown in Figure 1, and the basic model parameters are shown in Tables 1~2.

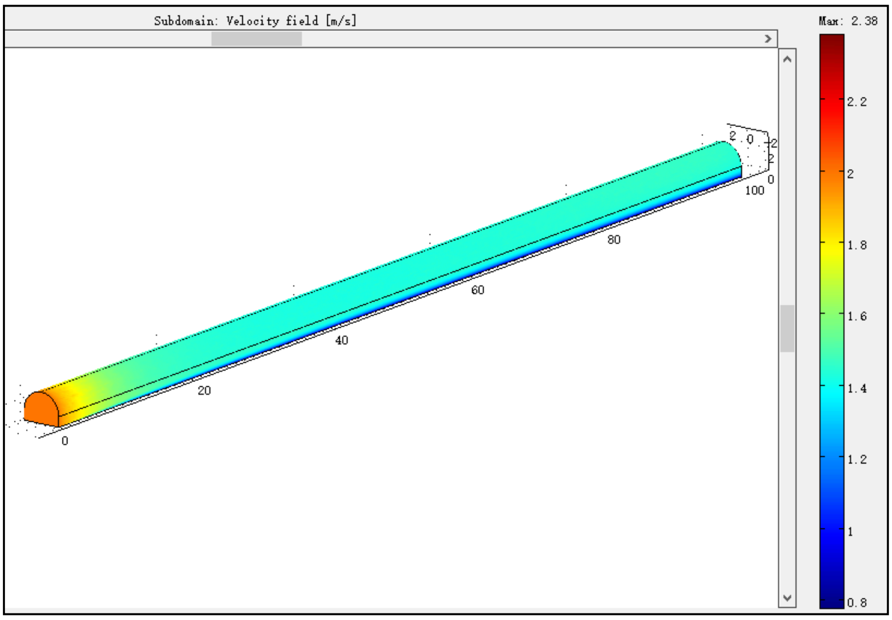

Figure 1. Model of half round arch tunnel

Table 1. Basic parameters for simulation of semi circular arch tunnels

Wind speed (m/s)	Hydraulic diameter (m)	ν (m^2/s)	Re_{D_H}	I %
0.8	3.44	14.4×10^{-6}	7.17×10^4	3.96
2	3.44	14.4×10^{-6}	1.91×10^5	3.50
4	3.44	14.4×10^{-6}	4.78×10^5	3.12
6	3.44	14.4×10^{-6}	9.56×10^5	2.86

Table 2. Values of roughness height as basic parameters for simulating semicircular arch tunnels

Support method	Hydraulic diameter (*m*)	$\alpha\times10^4$	Roughness height (*m*)	Roughness coefficient
Bolting and shotcreting	3.44	100	0.0253	0.5

4. Numerical Simulation Results and Analysis

4.1. Distribution characteristics of airflow field on the cross-section of the tunnel

Simulate the contour map of velocity distribution on the tunnel section according to the simulation plan. Select contour maps for wind speeds of 0.8m/s and 4.0m/s, as shown in Figure 2. In establishing a simplified velocity model, considering avoiding the influence of eddy currents in the tunnel flow field, the cross-sectional data at a distance of 50m from the tunnel entrance is selected as the basis. At this time, the airflow velocity field remains basically unchanged on the cross-section and reaches a fully developed state.

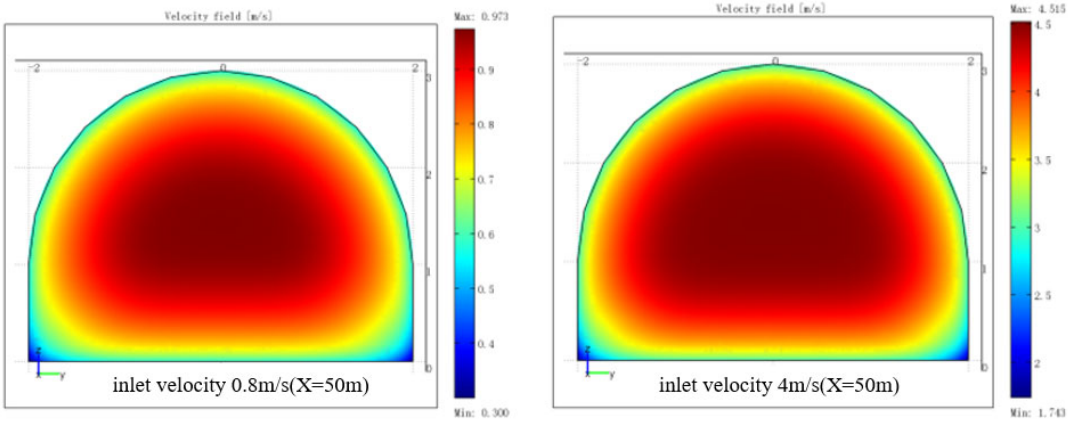

Figure 2. Contour map of velocity distribution on the cross-section of a semi circular arch roadway

From Figure 2, it can be seen that the contour line of the wind speed contour line of the tunnel section is consistent with the shape of the section, and the wind speed contour line is basically parallel to the tunnel wall. The wind speed contour line expands from the central part of the tunnel section to the tunnel wall. The closer the wind speed contour line is to the wall of the tunnel, the denser it is, indicating that the wind speed gradient is greater near the wall, and the more sparse the wind speed contour line is near the middle of the tunnel, indicating that the wind speed gradient is smaller and the central wind speed of the tunnel is basically equal. In the same tunnel, the higher the average wind speed, the smaller the thickness of the near wall velocity change layer, that is, the thickness of the boundary layer decreases with the increase of wind speed.

4.2. Wind speed distribution pattern on the central axis

Based on the distribution of cross-sectional wind speed at X=50m in the roadway, an empirical calculation formula for calculating the average wind speed of the roadway cross-section is obtained by calculating the point wind speed of the roadway cross-section. The relationship between the average wind speed and the roadway cross-section is found, and then Origin8.0 is used to fit the non-linear functions of point speed and average wind speed. According to the simulated plan, the type of tunnel selected is selected, and the data monitoring location is selected at X=50m of the tunnel. The central axis of the tunnel is the data monitoring line, and the wind speed on the central axis of the tunnel section is simulated for data analysis. The inlet wind speeds are taken as 0.8m/s, 2m/s, 4m/s, and 6m/s. The partial data of point velocity v and distance d at different inlet wind speeds are shown in Table 3, and the corresponding V-d diagram is shown in Figure 3.

Table 3. Partial data of point velocity v and distance d at different inlet wind speeds

d (m)	0	0.2	0.5	0.9	1.4	2	2.5	2.8	3
$v_{0.8}(m/s)$	0	0.74	0.85	0.94	0.97	0.96	0.87	0.76	0
$v_2(m/s)$	0	1.89	2.06	2.24	2.29	2.28	2.11	1.95	0
$v_4(m/s)$	0	3.79	4.13	4.45	4.51	4.49	4.21	3.88	0
$v_6(m/s)$	0	5.69	6.19	6.63	6.71	6.69	6.30	5.74	0

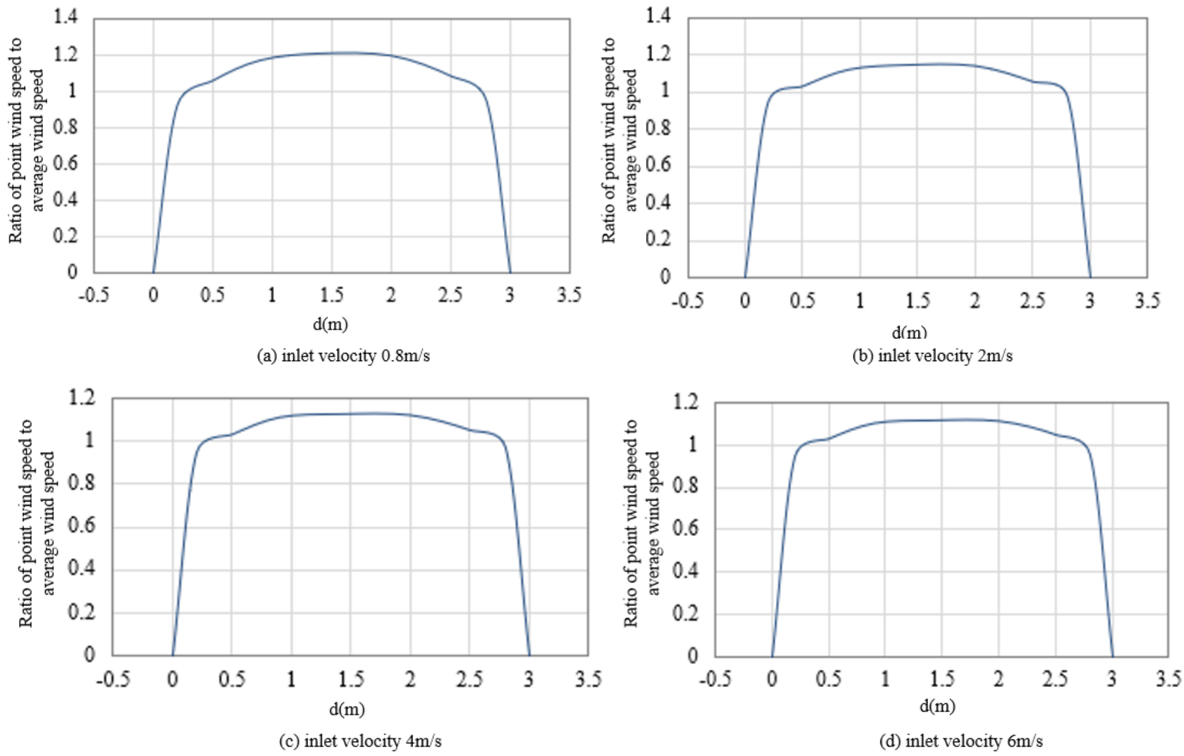

Figure 3. v-d diagram of point speed v changing with distance d at different wind speeds

(1) The inlet wind speed is 0.8m/s, when $d \subseteq [0,1.25]$, $v_{0.8} / \bar{v} = 1.173+0.153\ln d$; when $d \subseteq [1.25,1.5]$, $v_{0.8} / \bar{v} = 1.2125$.

(2) The inlet wind speed is 2m/s, when $d \subseteq [0,1.25]$, $v_2 / \bar{v} = 1.1157+0.1075\ln d$; when $d \subseteq [1.25,1.5]$, $v_2 / \bar{v} = 1.145$.

(3) The inlet wind speed is 4m/s, when $d \subseteq [0,1.25]$, $v_4 / \bar{v} = 1.1055+0.0975\ln d$; when $d \subseteq [1.25,1.5]$, $v_4 / \bar{v} = 1.1275$.

(4) The inlet wind speed is 6m/s, when $d \subseteq [0,1.25]$, $v_6 / \bar{v} = 1.0985+0.092\ln d$; when $d \subseteq [1.25,1.5]$, $v_6 / \bar{v} = 1.118$.

4.3. Comparison of numerical simulation and theoretical model results

There are seven indicators to analyze the relationship between wind speed and average wind speed: roadway width, roadway height, average wind speed, ratio of maximum wind speed to average wind speed, distance d from numerical simulation average wind speed line to roof, distance D from theoretical calculation average wind speed line to roof, and error between numerical simulation results and theoretical calculation results. Verify the reliability of the theoretical calculation model through comparative analysis. The comparison results are shown in Table 4.

Table 4. Comparison of theoretical model and numerical simulation results for semicircular arch tunnel

Average wind speed (*m/s*)	Maximum wind speed/average wind speed	Simulated average wind speed line to roof distance d (m)	Theoretical average wind speed line to roof distance D (m)	Error（$\left\|\frac{d-D}{D}\right\| \times 100\%$）
0.8	1.2125	0.3228	0.3347	3.56%
2.0	1.1450	0.3286	0.3347	1.84%
4.0	1.1275	0.3305	0.3347	1.25%
6.0	1.1180	0.3266	0.3347	2.42%

From Table 4, it can be seen that the distance between the average wind speed line of the semi circular arch tunnel and the roof is 10.76%~11.02% of the tunnel height. The error between the theoretical calculation results and the numerical simulation results is within 4%, which verifies the reliability of the numerical simulation results.

5. Conclusion

(1) The wind speed contour line on the cross-section of the semi circular arch tunnel is basically parallel to the tunnel wall. The wind speed gradient near the tunnel wall is large, while the wind speed gradient in the middle of the tunnel is small. The thickness of the boundary layer decreases with

increasing wind speed. The ratio of the maximum wind speed to the average wind speed of the tunnel section is approximately 1.2125.

(2) The distance between the average wind speed line of the semi circular arch tunnel and the roof is 10.76%~11.02% of the tunnel height, and the error between this simulation result and the theoretical calculation result is within 4%.

Acknowledgment

The study was supported by Tiandi Technology Co., Ltd. Technology Innovation and Entrepreneurship Fund Special Project (2022-2-TD-ZD010) and Key R&D Project of middling coal Science and Engineering Group Chongqing Research Institute Co., Ltd. (2022ZDXM09).

References

[1] Wang Guofa, Wang Hong, Ren Huaiwei, et al. 2025 Scenario objectives and development path of smart coal mines [J]. Journal of Coal Industry, 2018,43 (02): 295-305.

[2] Zhou Fubao, Wei Lianjiang, Xia Tongqiang, et al. Principles, key technologies, and preliminary implementation of intelligent ventilation in mines [J]. Journal of Coal Industry, 2020,45 (06): 2225-2235.

[3] Wang Heng, Qiu Liming, He Xueqiu, et al. Study on the distribution law of wind speed at the cross-section of coal mine tunnels under different factors [J]. Mining Research and Development, 2022,42 (07): 125-132.

[4] Guo Weizhou, Shen Bin, Wang Yang, et al. Construction and application of intelligent ventilation system in Hulusu Coal Mine [J]. Coal Mine Safety, 2022,53 (09): 233-238.

[5] Hu Jianhua, Zhao Yang, Zhou Tan, et al. Multiple factors affecting the distribution of wind speed on the cross-section of uneven roof tunnels [J]. Journal of Central South University, 2021,28 (07): 2067-2078.

[6] Hao Yuanwei, Chen Kaiyan, Jiang Zhongcheng, et al. Correction and processing of tunnel wind speed monitoring values based on CFD simulation [J]. Coal Mine Safety, 2011, 42 (02): 1-3+7.

[7] Li Yong, Chu Zhaoxiang, Ji Jianhu, et al. Numerical simulation of airflow and temperature fields in excavation tunnels [J]. Coal Science and Technology, 2014,42 (S1): 142-145+148.

[8] Zhao Wenhua. Numerical simulation of flow field distribution during ventilation process in coal mine tunnels [J]. Coal and Chemical Industry, 2017,40 (04): 74-75+79.

[9] Lu Guangli, Wu Zanlong, Zhao Jianfeng. Numerical simulation of airflow changes in tunnels at different turning angles [J]. Mining Research and Development, 2019, 39 (12): 116-121.

[10] Wang Hanfeng. Simulation study on positioning and monitoring of average wind speed points in Fluent tunnel cross-section [J]. Coal Science and Technology, 2015,43 (08): 92-96.

[11] Sun Liang, Sun Zhenping. Research on the distribution law and monitoring of wind speed in large section tunnels of mines [J]. Coal Technology, 2022,41 (04): 97-100.